Supporting Information

Feather light, mechanically robust cellulose ester aerogels for environmental remediation

Anurodh Tripathi[1,2], Greg N Parsons[1], Orlando J Rojas[1,2,3]* and Saad A. Khan[1]*

[1]Department of Chemical & Biomolecular Engineering, NC State University, 911 Partners Way, Engineering Building I (EB1) Raleigh, North Carolina 27695-7905, USA
[2]Department of Forest Biomaterials, NC State University, 2820 Faucette Drive, Biltmore Hall, Raleigh, North Carolina 27695-8005, USA
[3]Department of Byproducts and Biosystems, School of Chemical Engineering, Aalto University, Vuorimiehentie 1, P.O. Box 16300, FIN-00076 Aalto, Espoo, Finland

E-mail: khan@eos.ncsu.edu; ojrojas@ncsu.edu

Keywords: (cellulose acetate, cellulose acetate propionate, cellulose acetate butyrate, chemical vapor deposition, oil-spill)

---

[c]orresponding authors: khan@eos.ncsu.edu; ojrojas@ncsu.edu

Movie S1: Demonstration of separation of spent kerosene oil obtained from cleaning the pump.

Movie S2: Demonstration of separation of spent kerosene oil from oil in water stirred emulsion system.

Movie S3: Demonstration of separation of spent motor oil (obtained from the oil change) from water in a stirred system to model oil spill in a turbulent ocean.
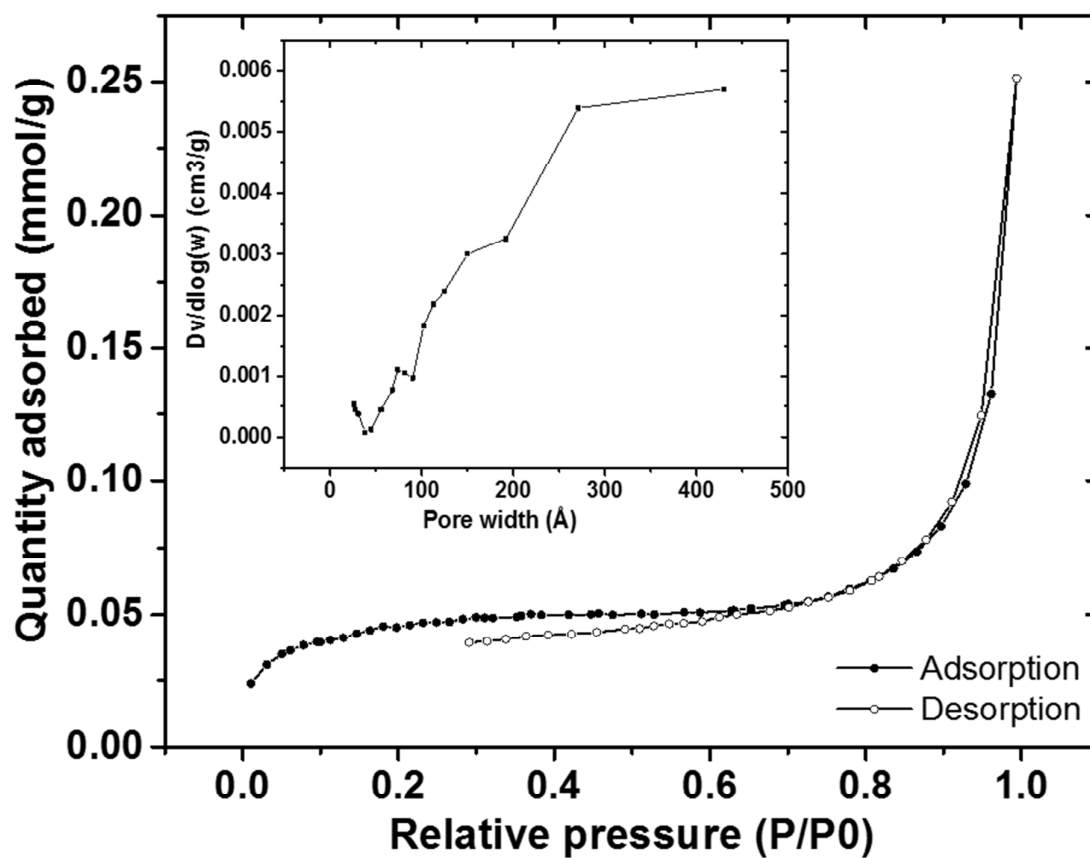
Figure S1: N$_2$ adsorption and desorption isotherm obtained for 4% CDA aerogel. Inset shows the pore size distribution derived from desorption curve of the isotherm by the Barrett-Joyner-Halenda (BJH) method.
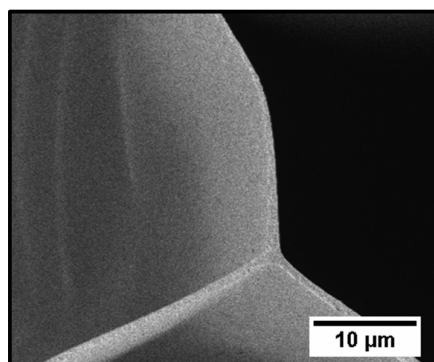

Figure S2: SEM image of the juction point at one pore in the aerogel. The wall thickness is ~1 μm.

Density calculations:

Organogel density: If there was no swelling or shrinkage during the solvent exchange and freeze drying step, the density can be calculated as follows

$$\rho_{organogel} = \frac{M_{CDA}}{\dfrac{M_{CDA}}{\rho_{CDA}} + \dfrac{(1 - M_{CDA})}{\rho_{water}}}$$

where, ρ_{cal} = calculated density of the aerogel,
      M_{CDA} = weight % of the CDA added for aerogel synthesis
      ρ_{CDA} = density of the cellulose diacetate flakes (1.3 g cm^{-3})
      ρ_{water} = density of DI water (0.998 g cm^{-3})

Hydrogel density: The hydrogel density is calculated by measuring volume of each hydrogel via volume displacement using deionized water in a flat based beaker. Assuming, there was no shrinkage during freeze drying, the hydrogel density is calculated as follows:

$$\rho_{hydrogel} = \frac{M_{CDA}}{V_{hydrogel}}$$

Surface area calculation for CDA aerogels: Assuming that the aerogel is composed of cylindrical pores with diameter ranging from 50-100 μm with wall thickness of 1 μm as seen from SEM, we can calculate the range of surface area as follows:

1 gm of 4% aerogel has volume $V = 1/\rho_{aerogel} = \dfrac{1}{0.0234} cm^3$

Total surface area $A = 2\pi r h N$ ---1

$V = \dfrac{1}{0.0234} = \pi r^2 h N + 2\pi r h N w$ ---2

From (1) & (2),

$$A = \frac{2}{0.0234(r + 2w)} m^2/g \quad = \quad 1.6 - 3.2 \text{ m}^2 \text{ g}^{-1}$$

where, r= pore size radius = 25-50 μm
        h = height of one cylindrical pore
        N = total number of pores
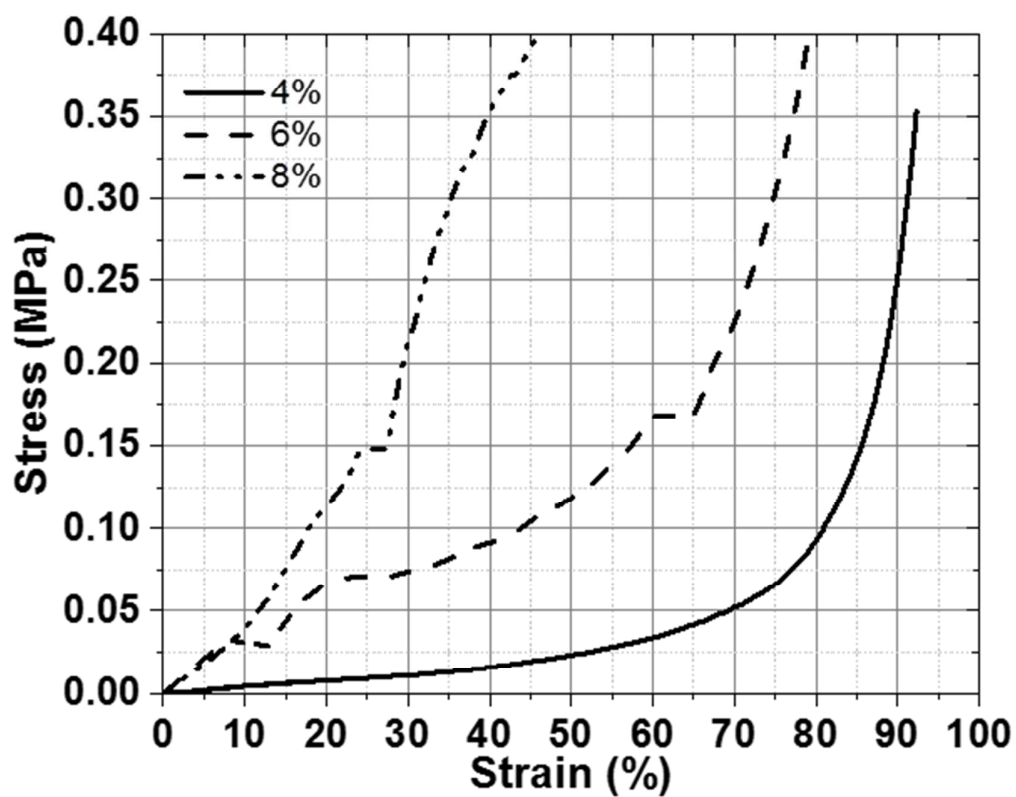   w = wall thickness of the pore ~ 1 μm

Figure S3: The compressive stress-strain curve for 4. 6, and 8% aerogels. The curves for 6 and 8% were not reproducible due to unavoidable artifacts generated during solvent exchange and freezing step. However, they consistently yielded below 30%.
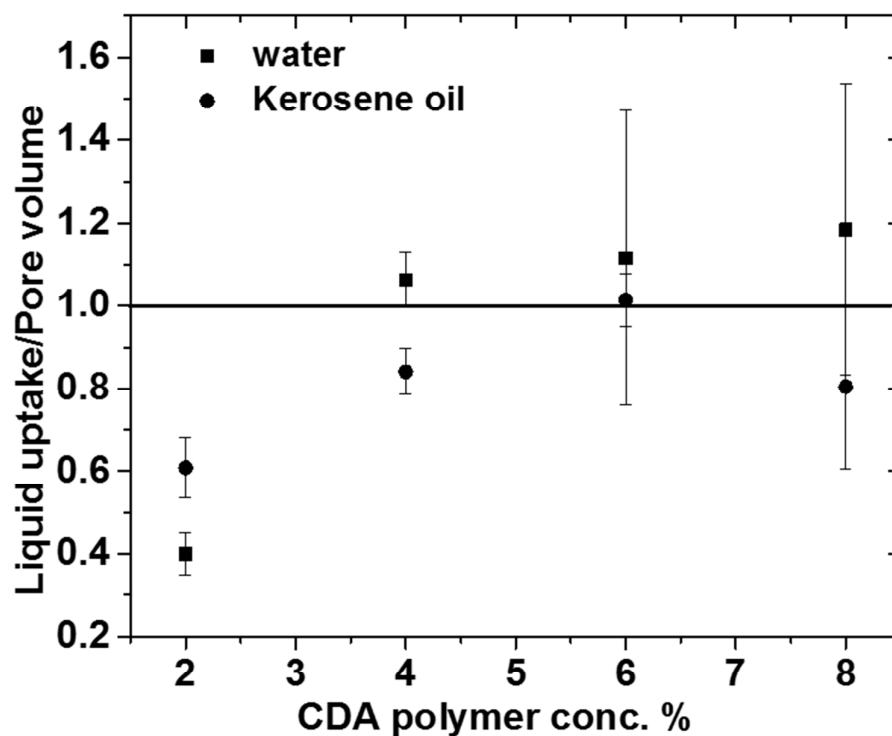
Figure S4: Liquid uptake w.r.t the available pore volume per gram of aerogel for 2, 4, 6 and 8 % aerogels. A ratio greater than 1 for water uptake by 4% and above aerogel indicates a combination of absorption in the pores and adsorption on the polymer walls may be due to hydrogen bonding of water with polymer chains. Hence the liquid uptake is referred to as sorption. The low value of sorption for 2% aerogel relative to the available pore volume is may be due to inability of 2% aerogel to retain such high volume of water. Relative volumetric uptake for kerosene oil is less than or equal to 1, which further implies entrapment of air bubbles during sorption.
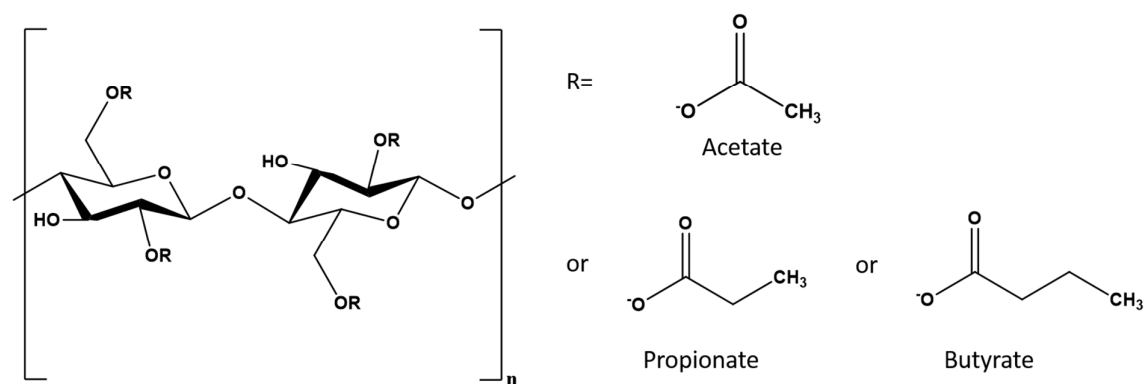
Figure S5: Chemical formulae for Cellulose diacetate (CDA), Cellulose Acetate Propionate (CAP) and Cellulose Acetate Butyrate (CAB).

Following categories of these polymers were used in the study: Cellulose diacetate (acetyl: 39.8%, hydroxyl: 3.5%), cellulose acetate propionate (propionyl: 42.5%, hydroxyl: 5%) and cellulose acetate butyrate (butyryl: 46%, hydroxyl: 4.8%)

X-ray Photospectroscopy (XPS) was done using SPECS FlexMod system with hemispherical analyzer PHOIBOS 150. The base pressure in the analysis chamber is in 10^{-10} mbar range. The samples were excited via Al kα excitation (1486.7 eV) with electron beam incident at ~30^0 from the surface. Energy calibration was established by referencing to adventitious carbon (C1s line at 285.0 eV binding energy). Survey scans were taken with 0.5 eV steps and 0.04 s dwell per point and Epass setting of 24. High resolution scans were taken with 0.1 eV steps and 0.5s dwell per point with Epass setting of 20.

Modified aerogel	Si/O %
Top	18.9
Middle	1.8

Table 1

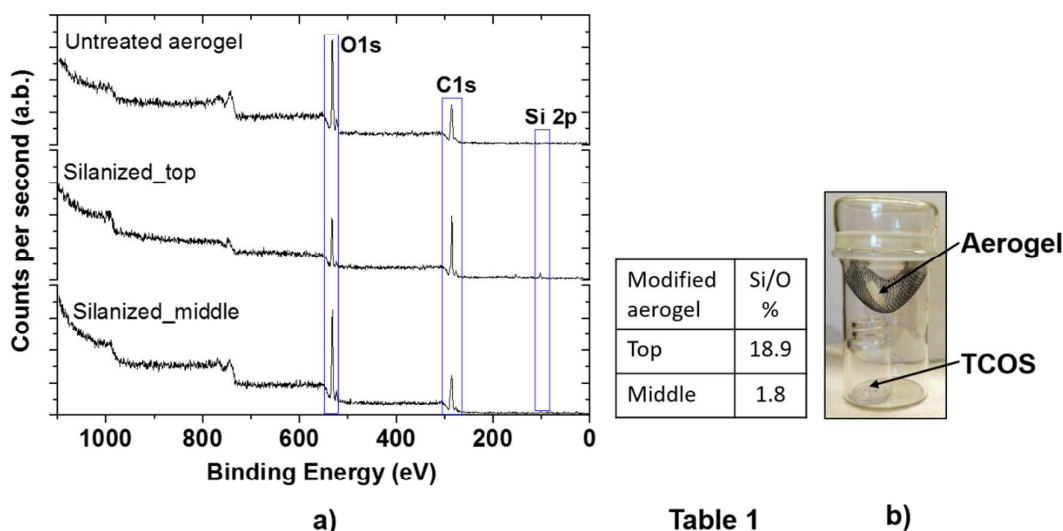a)   Table 1   b)

Figure S6: a) XPS survey scan for unmodified and modified aerogel (top & radial cross-section), b) a bottle in bottle set up used for chemical vapor deposition. Table1: Calculated Si/O% at the top and radial cross-section of modified aerogel as calculated from XPS.

Table S1: Material properties of the aerogels synthesized in current study and prior studies

	density (g/ml)	Compression Modulus (kPa)	Specific Modulus (MPa/g/ml)	Yield strain (%)	Highest strain (%)	Maximum compressive stress (kPa)	Maximum stress at 60% strain (kPa)	Reference
4% aerogel	0.0234	38	1.6	NA	92	350[1]	33.5	This work
CNF aerogel	0.0081	54.5	6.7	19	80	2	15	(Jiang & Hsieh, 2014)
CNC aerogel	0.0217	40	1.8	NA	80	7[1]	10	(Yang & Cranston, 2014)
Graphene	0.0058	2.3	0.4	NA	95	10[1]	1.5	(Xu et al., 2015)
Carbon nanofiber	0.006	10	1.7	NA	90	64[1]	6	(Wu, Li, Liang, Chen, & Yu, 2013)

[1] The materials showed no yield stress. Elastic region was followed by densification region. The values represent compressive stress, i.e., the stress at maximum strain

Table S2: Comparison with other studies on aerogels for oil sorption reported in literature

S.No.	Material	Preparation method	Conc. wt %	Bulk Density (mg/cc)	Porosity %	Sorption g/g		Reusability (# of times sorbed and desorbed)	Drawbacks	Reference
						water	Non polar solvent			
1.	Cellulose fiber (patent)	Freeze drying of cellulose suspension followed by CVD of silane	NA	40-80	94-98	5-25	10-25	3	Low sorption, high density compared to other aerogels,	(Duong, 2014)
2.	Cellulose nanofibril from rice straw (CNF)	TEMPO oxidation of CNF followed by freeze drying and CVD of silane	0.1 - 0.6	1.7-8.1	99.9-99.5	210	375	6	mechanical integrity in practical scenario is questionable, reusability is demonstrated by distilling toluene (not practical)	(Jiang & Hsieh, 2014)
3.	Nanocellulose	Freeze drying NFC dispersion in water followed by CVD of silane	0.5-2	4-14	99.8-99.5	NA	30-40	3	Complicated procedure for NFC production, mechanical integrity in practical situation is questionable	(Cervin, Aulin, Larsson, & Wågberg, 2012)
4.	Nanocellulose from birch kraft pulp	Freeze drying NFC hydrogels followed by CVD of silane	1.3	20	98.6	NA	NA	Not tested	Not tested for sorption applications	(Jin et al., 2011)
5.	Nanocellulose from hardwood kraft pulp	Freeze drying of nanocellulose hydrogel followed by TiO$_2$ Atomic layer deposition	2	20-30	98	NA	30	10	Reusability is demonstrated by evaporating Toluene (not practical)	(Korhonen, Kettunen, Ras, & Ikkala, 2011)
6.	Recycled cellulose fibers	Cellulose fiber dispersion freeze dried and CVD with silane	0.25-1	9-42	99.4-97.2	NA	45-62	Not tested	Very slow separation of oil and water, reusability not tested	(Feng, Nguyen, Fan, & Duong, 2015)
7.	Cellulose nanocrystal	Hydrazine cross-linking followed by freeze drying	0.5-2	5.6-21.7	99.6-98.6	72	160	20	Long and complicated synthesis procedure, not studied for oil separation	(Yang & Cranston, 2014)

#	Material	Method							Remarks	Reference
8.	Cellulose nanofibril	Kymene crosslinking followed by freeze drying	0.6-1	10-20	99.9-99.8	98	NA	Not tested	Not studied for oil separation	(Zhang, Zhang, Lu, & Deng, 2012)
9.	Bacterial cellulose	Liquid phase silanation followed by freeze drying	NA	6.77	99.6	NA	185	10	Very expensive material, long synthesis procedure, practical application not demonstrated	(Sai et al., 2015)
10	Carbon nanofiber	Bacterial cellulose aerogel via freeze drying followed by pyrolysis	NA	4-6	>99	NA	106-312	5	Material loss from pyrolysis, High temperature treatment	(Wu et al., 2013)
11	Graphene Framework	Hydrothermal treatment of Graphene oxide, freeze dried followed by pyrolysis	.035	2.1	>99	NA	200-600	Not tested	Material loss, expensive material, high temperature treatment	(Zhao et al., 2012)
12	Graphene and Carbon nanotube	Lyophilization of Carbon nanotube and graphene oxide followed by hydrazine vapor reduction	NA	0.16	>99	NA	580	10	Expensive raw material, practical use is questionable	(Sun, Xu, & Gao, 2013)
13	Chitosan-Silica	TEOS polycondensation in presence of chitosan followed by lyophilization	NA	5.8-17.3	96.7-90.9	NA	10-25	10	Low sorption, weak mechanical integrity, not suitable for practical use, reusability demonstrated by evaporation of solvent (not practical)	(Ma, Liu, Dong, Wang, & Hou, 2015)
14	Silica	Polycondensation of methyltrimethoxysilane followed by supercritical drying	NA	NA	NA	NA	15	Not tested	Low sorption, weak mechanical integrity, not suitable for practical use	(Venkateswara Rao, Hegde, & Hirashima, 2007)

15	Cellulose acetate	Organic gel formation by isocyanate crosslinking followed by supercritical drying	5-10	250-750	82-42	NA	NA	Not tested	High density and low porosity, not tested for sorption properties	(Fischer, Rigacci, Pirard, Berthon-Fabry, & Achard, 2006)
16	Cellulose Acetate	Sol-gel route to crosslink via ester linkage followed by solvent exchange with water to give hydrogel which is freeze dried and CVD of silane	2-8	4.0-110.2	99.7-91.2	10-92	5-112	7-10		This work

References

Cervin, N. T., Aulin, C., Larsson, P. T., & Wågberg, L. (2012). Ultra porous nanocellulose aerogels as separation medium for mixtures of oil/water liquids. *Cellulose, 19*, 401–410. doi:10.1007/s10570-011-9629-5

Duong, H. M. et al. (2014). A polysaccharide aerogel. WO2014/178797. doi:WO2014/178797

Feng, J., Nguyen, S. T., Fan, Z., & Duong, H. M. (2015). Advanced Fabrication and Oil Absorption Properties of Super-hydrophobic Recycled Cellulose Aerogels. *Chemical Engineering Journal*. doi:10.1016/j.cej.2015.02.034

Fischer, F., Rigacci, a., Pirard, R., Berthon-Fabry, S., & Achard, P. (2006). Cellulose-based aerogels. *Polymer*, *47*, 7636–7645. doi:10.1016/j.polymer.2006.09.004

Jiang, F., & Hsieh, Y.-L. (2014). Amphiphilic superabsorbent cellulose nanofibril aerogels. *Journal of Materials Chemistry A*, *2*, 6337–6342. doi:10.1039/c4ta00743c

Jin, H., Kettunen, M., Laiho, A., Pynnönen, H., Paltakari, J., Marmur, A., … Ras, R. H. a. (2011). Superhydrophobic and superoleophobic nanocellulose aerogel membranes as bioinspired cargo carriers on water and oil. *Langmuir*, *27*(14), 1930–1934. doi:10.1021/la103877r

Korhonen, J. T., Kettunen, M., Ras, R. H. a, & Ikkala, O. (2011). Hydrophobic nanocellulose aerogels as floating, sustainable, reusable, and recyclable oil absorbents. *ACS Applied Materials and Interfaces*, *3*, 1813–1816. doi:10.1021/am200475b

Ma, Q., Liu, Y., Dong, Z., Wang, J., & Hou, X. (2015). Hydrophobic and nanoporous chitosan-silica composite aerogels for oil absorption. *Journal of Applied Polymer Science*, *132*(15), n/a–n/a. doi:10.1002/app.41770

Sai, H., Fu, R., Xing, L., Xiang, J., Li, Z., Li, F., & Zhang, T. (2015). Surface Modification of Bacterial Cellulose Aerogels' Web-like Skeleton for Oil/Water Separation. *ACS Applied Materials & Interfaces*, *7*(13), 7373–7381. doi:10.1021/acsami.5b00846

Sun, H., Xu, Z., & Gao, C. (2013). Multifunctional, ultra-flyweight, synergistically assembled carbon aerogels. *Advanced Materials*, *25*(18), 2554–2560. doi:10.1002/adma.201204576

Venkateswara Rao, a., Hegde, N. D., & Hirashima, H. (2007). Absorption and desorption of organic liquids in elastic superhydrophobic silica aerogels. *Journal of Colloid and Interface Science*, *305*(1), 124–132. doi:10.1016/j.jcis.2006.09.025

Wu, Z.-Y., Li, C., Liang, H.-W., Chen, J.-F., & Yu, S.-H. (2013). Ultralight, flexible, and fire-resistant carbon nanofiber aerogels from bacterial cellulose. *Angewandte Chemie (International Ed. in English)*, *52*(10), 2925–9. doi:10.1002/anie.201209676

Xu, X., Li, H., Zhang, Q., Hu, H., Zhao, Z., Li, J., … Qiao, Y. (2015). 3D Graphene / Iron Oxide Aerogel Elastomer Deformable in a Magnetic Field, 3969–3977.

Yang, X., & Cranston, E. D. (2014). Chemically Cross-Linked Cellulose Nanocrystal Aerogels with Shape Recovery and Superabsorbent Properties. *Chemistry of Materials*, *35*(2), 6016–6025. doi:10.1021/cm502873c

Zhang, W., Zhang, Y., Lu, C., & Deng, Y. (2012). Aerogels from crosslinked cellulose nano/micro-fibrils and their fast shape recovery property in water. *Journal of Materials Chemistry*, *22*(2), 11642. doi:10.1039/c2jm30688c

Zhao, Y., Hu, C., Hu, Y., Cheng, H., Shi, G., & Qu, L. (2012). A versatile, ultralight, nitrogen-doped graphene framework. *Angewandte Chemie - International Edition*, *51*(45), 11371–11375. doi:10.1002/anie.201206554